

Single Higgs boson production at the ILC in the left-right twin Higgs model

Yao-Bei Liu^{1,2}, Zhen-Jun Xiao^{1,3a}

*1. Department of Physics and Institute of Theoretical Physics,
Nanjing Normal University, Nanjing 210023, P.R.China*

2. Henan Institute of Science and Technology, Xinxiang 453003, P.R.China and

*3. Jiangsu Key Laboratory for Numerical Simulation of Large Scale Complex Systems,
Nanjing Normal University, Nanjing 210023, P.R. China*

In this work, we analyze three dominant single SM-like Higgs boson production processes in the left-right twin Higgs model (LRTHM): the Higgs-strahlung (HS) process $e^+e^- \rightarrow Zh$, the vector boson fusion (VBF) process $e^+e^- \rightarrow \nu\bar{\nu}h$ and the associate production with top pair process $e^+e^- \rightarrow t\bar{t}h$ for three possible energy stages of the International Linear Collider (ILC), and compared our results with the expected experimental accuracies for various accessible Higgs decay channels. The following observations have been obtained: (i) In the reasonable parameter space, the LRTHM can generate moderate contributions to these processes with polarized beams; (ii) Among various Higgs boson decay channels, the $b\bar{b}$ signal strength is most sensitive to the LRTHM due to the high expected precision. For the $t\bar{t}h$ production process, the absolute value of $\mu_{b\bar{b}}$ may deviate from the SM prediction by over 8.7% and thus may be detectable at the future ILC with $\sqrt{s} = 1$ TeV; (iii) The future ILC experiments may give strong limit on the scale parameter f : for the case of ILC-250 GeV, for example, the lower limit for parameter f of the LRTHM is $f > 1150$ GeV at the 2σ level.

PACS numbers: 12.60.Fr, 13.66.Jn, 14.80.Bn.

^a Email: xiaozhenjun@njnu.edu.cn

I. INTRODUCTION

On July 4th, 2012, a neutral Higgs boson with a mass around 125 GeV was discovered at CERN's Large Hadron Collider (LHC) by both the ATLAS and CMS collaborations [1, 2], whose properties appear to be well consistent with those expected of the Standard Model (SM) [3, 4]. However, the SM suffers from the so-called little hierarchy problem [5] and cannot provide a dark matter (DM) candidate, which is actually a sound case for new physics (NP) beyond the SM. On the other hand, the Higgs-like resonance with mass about 125 GeV can also be well explained in many NP models where the Higgs is a pseudo-Goldstone boson. Here we focus on the left-right twin Higgs model (LRTHM) [6, 7], which can successfully solve the little hierarchy problem and also predicts a good candidate for weakly interacting massive particle (WIMP) dark matter.

As we know, the precision measurements of the Higgs boson are rather challenging at the LHC, since various Higgs couplings to SM fermions and vector bosons still have large uncertainties based on the current LHC data [8]. Thus the most precise measurements will be performed in the clean environment of a future high energy e^+e^- linear collider, such as the International Linear Collider (ILC) [9, 10]. Furthermore, a unique feature of the ILC is the presence of initial state radiation (ISR) and beamstrahlung, which can help to improve the measurement precision. The ILC is planned to operate at three stages for the center-of-mass (c.m.) energy: 250 GeV, 500 GeV and 1 TeV. At the different energy stages, the Higgs-strahlung (HS) process $e^+e^- \rightarrow Zh$, the vector boson fusion (VBF) process $e^+e^- \rightarrow \nu\bar{\nu}h$, and the associated with top pair process $e^+e^- \rightarrow t\bar{t}h$ are three main production channels for the Higgs boson, which are very important for studying the properties of Higgs boson and testing NP beyond the SM [11]. These processes have been studied in the context of the SM [12, 13] and various NP models, such as the MSSM [14], the little Higgs models [15] and other composite Higgs models [16].

The LRTHM predicted the existence of the new heavy gauge bosons, top partner, neutral and charged scalars at or below the TeV scale, which can produce rich phenomenology at the high energy colliders [17–23]. In the LRTHM, the couplings of the electroweak gauge bosons to top quarks and the couplings of the SM-like Higgs boson to ordinary particles are corrected at the order $\mathcal{O}(v^2/f^2)$. Besides, the new particles, such as the heavy neutral gauge boson and top partner, can also contribute to some Higgs boson production processes. On the other hand, the decays $h \rightarrow gg, \gamma\gamma$, and $Z\gamma$ all receive contributions from the modified Higgs couplings and the new heavy particles, which has been studied in our recent work [24]. The aim of this paper is to consider the processes $e^+e^- \rightarrow Zh$, $e^+e^- \rightarrow \nu\bar{\nu}h$ and $e^+e^- \rightarrow t\bar{t}h$ in the LRTHM, and see whether the effects of this model on these processes can be detected in the future ILC experiments.

The paper is organized as follows. In section II, we recapitulate the LRTHM and lay out the couplings of the particles relevant to our calculation. In Sec. III, we study the effects of the LRTHM on three single Higgs boson production processes and project limits on the LRTHM from the future measurements of the 125 GeV Higgs at the ILC with polarized beams. Finally, we give our conclusion in Sec. IV.

II. RELEVANT COUPLINGS IN THE LRTHM

The twin Higgs mechanism was proposed as an interesting solution to the little hierarchy problem, which can be implemented in left-right model with the additional discrete symmetry being identified with left-right symmetry [6]. Here we will briefly review the essential features of this model and focus on the couplings relevant to our work. For more details of the LRTHM, one can see Ref. [17] and references therein.

The LRTHM has the gauged $SU(2)_L \times SU(2)_R \times U(1)_{B-L}$ sub-groups of the global $U(4) \times U(4)$ symmetry. The left-right symmetry implies that the gauge couplings of $SU(2)_L$ and $SU(2)_R$ are identical ($g_{2L} = g_{2R} = g$). Two Higgs fields (H and \hat{H}) are introduced in the LRTHM, and each transforms as $(4, 1)$ and $(1, 4)$, respectively under the global symmetry. They can be written as

$$H = \begin{pmatrix} H_L \\ H_R \end{pmatrix}, \quad \hat{H} = \begin{pmatrix} \hat{H}_L \\ \hat{H}_R \end{pmatrix}, \quad (1)$$

where $H_{L,R}$ and $\hat{H}_{L,R}$ are two component objects which are charged under the $SU(2)_L \times SU(2)_R \times U(1)_{B-L}$ as

$$H_L \text{ and } \hat{H}_L : (2, 1, 1), \quad H_R \text{ and } \hat{H}_R : (1, 2, 1). \quad (2)$$

The global $U(4)_1(U(4)_2)$ symmetry is spontaneously broken down to its subgroup $U(3)_1(U(3)_2)$ with non-zero vacuum expectation values(VEV):

$$\langle H \rangle = (0, 0, 0, f)^T, \quad \langle \hat{H} \rangle = (0, 0, 0, \hat{f})^T, \quad (3)$$

The spontaneous symmetry breaking results in 14 Nambu-Goldstone bosons, which can be parameterized as described in Ref. [17]. The gauge symmetry $SU(2)_L \times SU(2)_R \times U(1)_{B-L}$ is eventually broken down to $U(1)_{EM}$. Six Goldstone bosons are eaten by the SM gauge bosons (W^\pm, Z) and by the heavy gauge bosons (W_H^\pm, Z_H). Here W_H^\pm and Z_H are three additional gauge bosons with masses of a few TeV in this model. The remaining eight scalars include: one SM-like Higgs boson h , one neutral pseudoscalar ϕ^0 , a pair of charged scalar ϕ^\pm , and a $SU(2)_L$ doublet $\hat{h} = (\hat{h}_1^+, \hat{h}_2^0)$. Noticed that a parity is introduced in this model under which \hat{H} is odd while all other fields are even, which forbids renormalizable couplings between \hat{H} and fermions. The lightest particle in the odd \hat{h}_2^0 is stable and can be treated as a candidate for dark matter, which has been studied in Ref.[25].

Besides the new heavy gauge bosons, a pair of vector-like quarks are also introduced to cancel the one-loop quadratic divergence of Higgs mass. The masses of the heavy gauge bosons, SM-like top quark and top partner are given by [17]

$$m_{Z_H}^2 = \frac{e^2 C_W^2}{2S_W^2 C_{2W}} (f^2 + \hat{f}^2) - M_Z^2, \quad (4)$$

$$M_{W_H}^2 = \frac{1}{2} g^2 (\hat{f}^2 + f^2 \cos^2 x), \quad (5)$$

$$m_t^2 = \frac{1}{2} (M^2 + y^2 f^2 - N_t), \quad (6)$$

$$m_T^2 = \frac{1}{2} (M^2 + y^2 f^2 + N_t), \quad (7)$$

with $N_t = \sqrt{(M^2 + y^2 f^2)^2 - y^4 f^4 \sin^2 2x}$ and $x = v/(\sqrt{2}f)$. The values of the energy scales f and \hat{f} are interconnected once we set $v \simeq 246$ GeV. The parameter M is essential to the mixing between the SM-like top quark t and its partner T . The value of y can be determined by fitting the experimental value of the SM-like top quark mass m_t . The abbreviations S_W , C_W and C_{2W} in Eq. (4) are defined in the following way:

$$S_W = \sin \theta_W = \frac{g'}{\sqrt{g^2 + 2g'^2}}, \quad C_W = \cos \theta_W = \sqrt{\frac{g^2 + g'^2}{g^2 + 2g'^2}}, \quad C_{2W} = \cos 2\theta_W, \quad (8)$$

where θ_W is the well-known Weinberg angle. The unit of the electric charge can then be written in the form of $e = gS_W = gg'/\sqrt{g^2 + 2g'^2}$.

The relevant couplings for the vertices in the LRTHM used in this work are given as follows [17]:

$$g_L^{Zt\bar{t}} = \frac{eC_L S_L}{2S_W C_W}, \quad g_R^{Zt\bar{t}} = \frac{ef^2 x^2 S_W C_R S_R}{2\hat{f}^2 C_W^3}, \quad (9)$$

$$g_L^{Z_H t\bar{t}} = \frac{eC_L S_L S_W}{2C_W \sqrt{C_{2W}}}, \quad g_R^{Z_H t\bar{t}} = -\frac{eC_W C_R S_R}{2S_W \sqrt{C_{2W}}}, \quad (10)$$

$$g_L^{Z_H e^+ e^-} = \frac{2eS_W}{4C_W \sqrt{C_{2W}}}, \quad g_R^{Z_H e^+ e^-} = \frac{e(1 - 3C_{2W})}{4S_W C_W \sqrt{C_{2W}}}, \quad (11)$$

$$V_{\phi^0 t\bar{t}} = -\frac{iy}{\sqrt{2}} S_L S_R, \quad V_{h\phi^0 Z_\mu} = \frac{ie x}{6S_W C_W} p_{Z\mu}, \quad (12)$$

$$V_{ht\bar{t}} = -\frac{y}{\sqrt{2}} [(C_L S_R + S_L C_R x) P_L + (C_L S_R x + S_L C_R) P_R], \quad (13)$$

$$V_{hZ_{H_\mu} Z_{H_\nu}} = -\frac{e^2 f x}{\sqrt{2} S_W^2 C_W^2} g_{\mu\nu}, \quad V_{hZ_\mu Z_{H_\nu}} = \frac{e^2 f x}{\sqrt{2} C_W^2 \sqrt{C_{2W}}} g_{\mu\nu}, \quad (14)$$

with

$$S_L = \frac{1}{\sqrt{2}} \sqrt{1 - (y^2 f^2 \cos 2x + M^2)/N_t}, \quad C_L = \sqrt{1 - S_L^2}, \quad (15)$$

$$S_R = \frac{1}{\sqrt{2}} \sqrt{1 - (y^2 f^2 \cos 2x - M^2)/N_t}, \quad C_R = \sqrt{1 - S_R^2}. \quad (16)$$

Here the momentum p_Z in the coupling $V_{h\phi^0 Z}$ in Eq. (12) refers to the incoming momentum of Z boson.

In the LRTHM, the normalized couplings of $h f \bar{f}$ ($f = b, c$), $ht\bar{t}$, $h\tau^+\tau^-$, hVV^* ($V = Z, W$), hgg , and $h\gamma\gamma$ are given by [17, 23]:

$$V_{hVV}/\text{SM} \equiv \frac{V_{HVV}}{V_{HVV}^{\text{SM}}} = 1 - \frac{v^2}{6f^2}, \quad (17)$$

$$V_{h\tau^+\tau^-}/\text{SM} = \frac{V_{h\tau^+\tau^-}}{V_{h\tau^+\tau^-}^{\text{SM}}} = 1 - \frac{2v^2}{3f^2}, \quad V_{ht\bar{t}}/\text{SM} = C_L C_R, \quad (18)$$

$$V_{hgg}/\text{SM} = \frac{\frac{1}{2}F_{1/2}(\tau_t)y_t + \frac{1}{2}F_{1/2}(\tau_T)y_T}{\frac{1}{2}F_{1/2}(\tau_t)}, \quad (19)$$

$$V_{h\gamma\gamma}/\text{SM} = \frac{\frac{4}{3}F_{1/2}(\tau_t)y_t + \frac{4}{3}F_{1/2}(\tau_T)y_T + F_1(\tau_W)y_W}{\frac{4}{3}F_{1/2}(\tau_t) + F_1(\tau_W)}, \quad (20)$$

with

$$F_1 = 2 + 3\tau + 3\tau(2 - \tau)f(\tau), \quad F_{1/2} = -2\tau[1 + (1 - \tau)f(\tau)], \\ f(\tau) = [\sin^{-1}(1/\sqrt{\tau})]^2, \quad g(\tau) = \sqrt{\tau - 1} \sin^{-1}(1/\sqrt{\tau}), \quad (21)$$

for $\tau_i = 4m_i^2/m_h^2 \geq 1$. The relevant couplings y_t and y_T can be written as

$$y_t = S_L S_R, \quad y_T = \frac{m_t}{m_T} C_L C_R, \quad (22)$$

which can be determined by the parameters f and M . Here we have neglected the contributions from W_H and ϕ^\pm for the $h \rightarrow \gamma\gamma$ decay, this is because their contributions are even much smaller than that for the T -quark [24]. On the other hand, the relation between G_F and v is modified from its SM form, introducing an additional correction y_{G_F} as $1/v^2 = \sqrt{2}G_F y_{G_F}^2$ with $y_{G_F}^2 = 1 - v^2/(6f^2)$.

III. NUMERICAL RESULTS AND DISCUSSIONS

In the LRTHM, the tree-level Feynman diagrams of the processes $e^+e^- \rightarrow Zh$, $e^+e^- \rightarrow \nu\bar{\nu}h$, and $e^+e^- \rightarrow t\bar{t}h$ are shown in Figs. 1-2. We can see that the modified couplings of hXX and the additional particles (Z_H and T -quark) can contribute to these processes at the tree level.

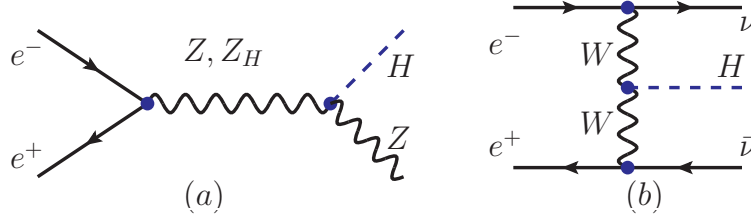


FIG. 1. Feynman diagrams for the Higgs-strahlung process $e^+e^- \rightarrow Zh$ (left) and WW -fusion process $e^+e^- \rightarrow \nu\bar{\nu}h$ (right).

Obviously, the heavy T -quark, the neutral scalar ϕ^0 and the charged Higgs bosons ϕ^\pm can also contribute to these processes at the loop level. However, their loop contributions are all most possibly very small and can be neglected due to the following two reasons:

- (i) The T -quark is very heavy and meanwhile the couplings of $hT\bar{T}$ is very small as shown in Ref. [17].
- (ii) The couplings of $h\phi^0\phi^0$ and $h\phi^+\phi^-$ are both suppressed largely by a factor of $v^2/(2f^2) < 0.08$.

We therefore only focus on those tree contributions at the lowest-order in this work. We will evaluate the relevant loop contributions in the near future to examine the smallness of the loop contributions directly.

In our numerical calculations, the SM-like Higgs boson mass is fixed as 125 GeV, the SM input parameters involved are taken from [26]. Besides, there are two LRTHM parameters: f and M . The indirect constraints on f come from the Z -pole precision measurements, the low energy neutral current process and the high energy precision measurements off the Z -pole: all these data prefer the parameter f to be larger than 500-600 GeV [17]. The mixing parameter M also be constrained by the $Z \rightarrow b\bar{b}$ branching ratio and oblique parameters [17, 18].

In the LRTHM, furthermore, the masses of heavy neutral gauge boson Z' and top partner T are determined by the given values of f and M . Currently, the masses of the new heavy particles, such

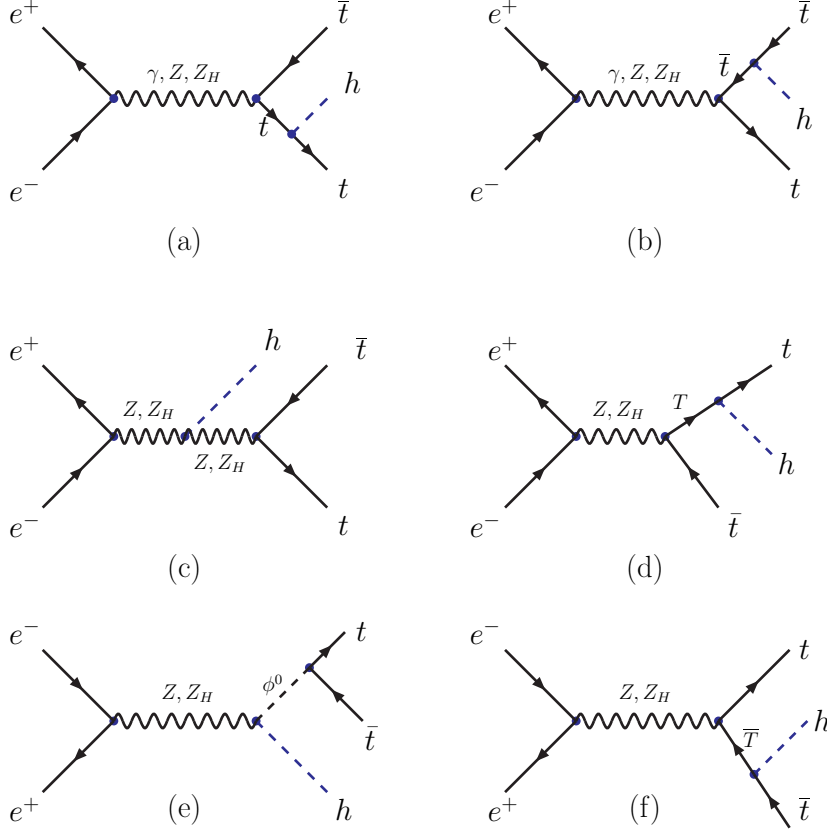


FIG. 2. Feynman diagrams for the process $e^+e^- \rightarrow t\bar{t}h$ in the LRTHM.

as the Z' and T have been constrained by the LHC experiments, as described in Refs. [27, 28]. In other words, the LHC data also imply some indirect constraints on the allowed ranges of both the parameters f and M through their correlations with $m_{Z'}$ and m_T , as discussed in Ref. [24]. For example, the top partner T with mass below 656 GeV are excluded at 95% confidence level according to the ATLAS data [29] if one takes the assumption of a branching ratio $BR(T \rightarrow W^+b) = 1$. The ATLAS [30] and CMS [31] collaborations have excluded the leptophobic Z' boson with the mass smaller than 1.32 TeV (ATLAS) and 1.3 TeV (CMS). A Z' in the LRTHM with a mass below 940 GeV has been excluded in Ref. [34] by using the D0 and CDF measurements. By taking the above constraints from the electroweak precision measurements and the LHC data into account, we here assume that the values of the parameter f and M are in the ranges of

$$600\text{GeV} \leq f \leq 1500\text{GeV}, \quad 0 \leq M \leq 150\text{GeV}, \quad (23)$$

in our numerical evaluations.

From Fig.2(e) we can see that the neutral scalar ϕ^0 can also contribute to the cross section. However, this contribution is very small due to the suppressed couplings of $h\phi^0 Z$ and $\phi^0 t\bar{t}$, and thus we can safely take its mass as $m_{\phi^0} = 150$ GeV. All the numerical evaluations have been done by using the CalcHEP package [35].

A. The production cross section with polarized beams

As is well-known, beam polarization is an essential ingredient at future high-energy linear collider experiments. Since the electrons and positrons in the beams are essentially chirality eigenstates, appropriate beam polarization in some processes can greatly increase the new physics signals and reduce the SM background [36]. With the longitudinal polarization of the initial electron and positron beams, the cross section of a process can be expressed as [37]

$$\sigma(P_{e^-}, P_{e^+}) = \frac{1}{4}[(1 + P_{e^-})(1 + P_{e^+})\sigma_{RR} + (1 - P_{e^-})(1 - P_{e^+})\sigma_{LL} + (1 + P_{e^-})(1 - P_{e^+})\sigma_{RL} + (1 - P_{e^-})(1 + P_{e^+})\sigma_{LR}], \quad (24)$$

where P_{e^-} (P_{e^+}) is the polarization degree of the electron (positron) beam. σ_{LR} stands for the cross section for completely left-handed polarized e^- beam ($P_{e^-} = -1$) and completely right-handed polarized e^+ beam ($P_{e^+} = 1$), and other cross sections σ_{LL} , σ_{RR} , and σ_{RL} are defined analogously.

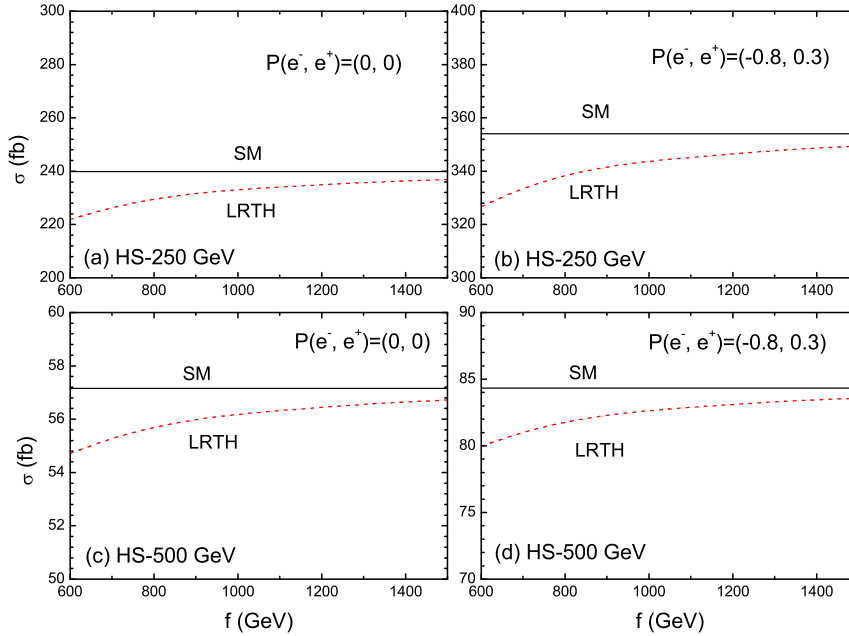


FIG. 3. The cross sections σ versus the scale f at the ILC with unpolarized and polarized beams for HS process with $M = 150$ GeV.

In Figs. 3 and 4, we plot the production cross sections for three processes $e^+e^- \rightarrow (Zh, \nu\bar{\nu}h, t\bar{t}h)$ with $\sqrt{s} = 250, 500$ GeV and 1000 GeV at the ILC in the SM and LRTHM. One can see that the cross sections in LRTHM are always smaller than those in the SM, and the values of cross sections increase as the parameter f increases, which means that the correction of the LRTHM decouples with the scale f increasing. This is similar with the situation in the little Higgs models [38, 39]. For comparison we also show the corresponding results for unpolarized beams. One can see that the cross sections with polarized beams are always larger than those with the unpolarized beams, and thus make the ILC more powerful in probing such new physics effects.

For HS process, the Feynman diagram involving s -channel gauge bosons exchange have more contributions to σ_{LR} than to σ_{RL} , this is because the neutral gauge bosons do not couple to $e_R^- e_R^+$

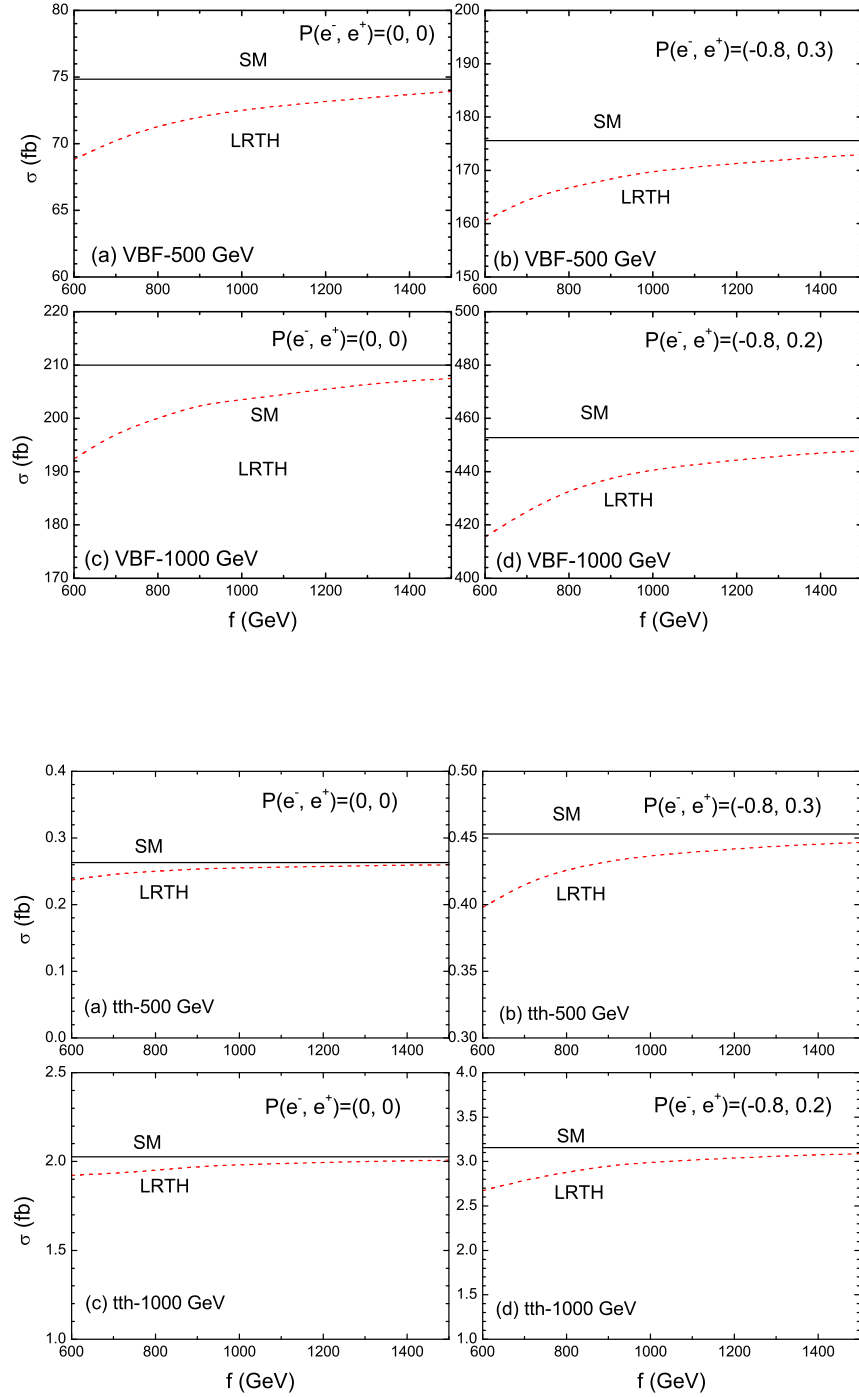


FIG. 4. The same as Fig. 3, but for the case of VBF and $t\bar{t}h$ processes.

and $e_L^- e_L^+$, while the couplings to $e_L^- e_R^+$ are stronger than those to $e_R^- e_L^+$. For the case of the unpolarized beams with $\sqrt{s} = 250(500)$ GeV, the cross section of the HS process is about 240 (57) fb, which is similar with the results in Refs. [40]. At low energy (such as $\sqrt{s} = 250$ GeV), the HS process is dominant and the cross section can reach about 350 fb for the case of the polarized beams, while the VBF and $t\bar{t}h$ processes are more significant at higher energies.

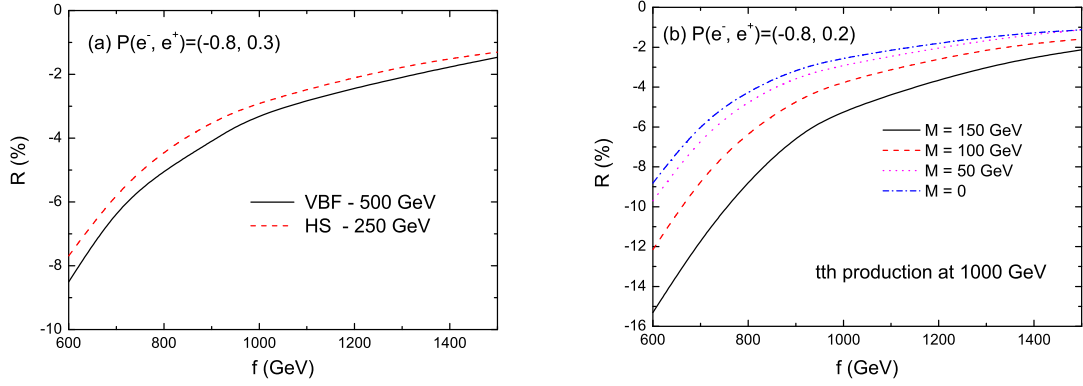


FIG. 5. The relative correction parameter $R = (\sigma^{\text{LRTHM}} - \sigma^{\text{SM}})/\sigma^{\text{SM}}$ versus the scale f at the ILC with polarized beams for three processes.

In Fig. 5, we show the f -dependence of the relative correction parameter $R = (\sigma^{\text{LRTHM}} - \sigma^{\text{SM}})/\sigma^{\text{SM}}$ for three production channels with polarized beams. For the considered three processes, the relative corrections are all negative and has a moderate dependence on the variations of the scale parameter f . The absolute values of suppression are larger than 5% for small values of f , but become smaller for larger values of the scale f . The total SM electroweak correction for the HS production process is about 5% for $m_h = 125$ GeV and $\sqrt{s} = 250$ GeV [12]. The expected accuracies for HS and VBF processes are about $2.0 \sim 2.6\%$ for $m_h = 125$ GeV [10]. For the process $e^+e^- \rightarrow t\bar{t}h$, the relative corrections are sensitive to the variations of the parameters M and f , and become larger in size for larger M and smaller f . For $M = 150$ GeV and $f \leq 800$ GeV, for example, the NP contribution can alter the SM cross section over 8%. At the ILC with $\sqrt{s} = 1000$ GeV, an accuracy of about 6.3% could be reached with the polarized beams [10]. The new physics effects considered here therefore might be detected in the future high precision ILC experiments.

B. The Higgs signal strengths

Considering the Higgs boson decay channels, the Higgs signal strengths can be defined as

$$\mu_i = \frac{\sigma_{\text{LRTHM}} \times BR(h \rightarrow i)_{\text{LRTHM}}}{\sigma_{\text{SM}} \times BR(h \rightarrow i)_{\text{SM}}}, \quad (25)$$

where i denotes a possible final state of the Higgs boson decay (for example $b\bar{b}$, gg , $c\bar{c}$, ZZ^* and $\gamma\gamma$). The projected 1σ sensitivities of the relevant channels at the ILC are shown in Table I. We can see that the $b\bar{b}$ channel is more easily accessible than other channels.

In the LRTHM, the modifications of the hVV ($V = Z, W$) and $hf\bar{f}$ (the SM fermions pair) couplings can give the extra contributions to the Higgs boson production processes. On the other hand, the loop-induced couplings, such as $h\gamma\gamma$ and hgg , could also be affected by the presence of top partner, new heavy charged gauge bosons and charged scalars running in the corresponding loop diagrams. Finally, beside the effects already seen in the HS channel due to the exchange

TABLE I. Projected 1σ sensitivities of various channels for the ILC operating at $\sqrt{s} = 250$ GeV, 500 GeV and 1000 GeV, respectively [10, 41].

\sqrt{s} (P_{e^-}, P_{e^+})	250 GeV (-0.8, 0.3)		500 GeV (-0.8, 0.3)			1 TeV (-0.8, 0.2)	
channel	HS	VBF	HS	VBF	ttH	VBF	ttH
$h \rightarrow b\bar{b}$	1.1%	10.5%	1.8%	0.66%	35%	0.47%	8.7%
$h \rightarrow gg$	9.1%	-	14%	4.1%	-	3.1%	-
$h \rightarrow c\bar{c}$	7.4%	-	12%	6.2%	-	7.6%	-
$h \rightarrow \tau^+\tau^-$	4.2%	-	5.4%	14%	-	3.5%	-
$h \rightarrow ZZ^*$	19%	-	25%	8.2%	-	4.4%	-
$h \rightarrow WW^*$	9.1%	-	9.2%	2.6%	-	3.3%	-
$h \rightarrow \gamma\gamma$	34%	-	34%	23%	-	8.5%	-

of s -channel heavy neutral gauge boson Z_H , the exchange of top partner T could also affect the production cross section for the process $e^+e^- \rightarrow t\bar{t}h$. All these effects can modify the signal strengths in a way that may be detectable at the future ILC experiments.

In Fig. 6, we show the dependence of the Higgs signal strengths μ_i ($i = b\bar{b}, gg$) on the parameter f and M for the HS and VBF processes with polarized beams, where (a) and (c) denote the Higgs signal strengths $\mu_{b\bar{b}}$ while (b) and (d) denote μ_{gg} . One can see that (i) the NP correction becomes smaller rapidly along with the increase of the scale f . (ii) For the HS process, the contributions of the LRTHM can be detected by the measurement of the $b\bar{b}$ signal rate in the future ILC experiments. However, it is difficult to observe these effects via the gg channel due to the relative weak bound. (iii) For the VBF process, the contribution of the LRTHM can be easily detected by the measurement of the $b\bar{b}$ signal rate due to the high expected precision. Meanwhile, this contribution can also be detected by the measurement of the gg signal rates in most part of the parameter spaces.

In Fig. 7, we show the dependence of the Higgs signal strengths $\mu_{b\bar{b}}$ on the parameter f and M for the process $e^+e^- \rightarrow t\bar{t}h$. From Table I we know that the 35% accuracy for top Yukawa couplings expected at $\sqrt{s} = 500$ GeV can be improved to the level of 8.7% at $\sqrt{s} = 1$ TeV. Only for $f = 600$ GeV and $M = 150$ GeV, the Higgs signal strengths $\mu_{b\bar{b}}$ can reach 0.84 for $\sqrt{s} = 500$ GeV. Thus it is difficult to observe the LRTHM effect on this process at $\sqrt{s} = 500$ GeV via the $b\bar{b}$ channel. For $\sqrt{s} = 1$ TeV, however, one can see the magnitude of such correction becomes more sizable for larger M and lower values of the scale f . For example, for $M = 150$ GeV and $f \leq 800$ GeV, the absolute value of $\mu_{b\bar{b}}$ can deviate from the SM prediction by over 9%, which might be detected in the future ILC experiments.

C. Simulated expectations at the ILC

Now we perform a simulation by using the projected 1σ sensitivities for the channels in the HS and VBF processes at the ILC-250 GeV, ILC-500 GeV, and ILC-1000 GeV respectively, as listed in Table I [10, 41]. The χ^2 function can be defined as

$$\chi^2 = \sum_i \frac{(\mu_i - 1)^2}{\sigma_i^2}, \quad (26)$$

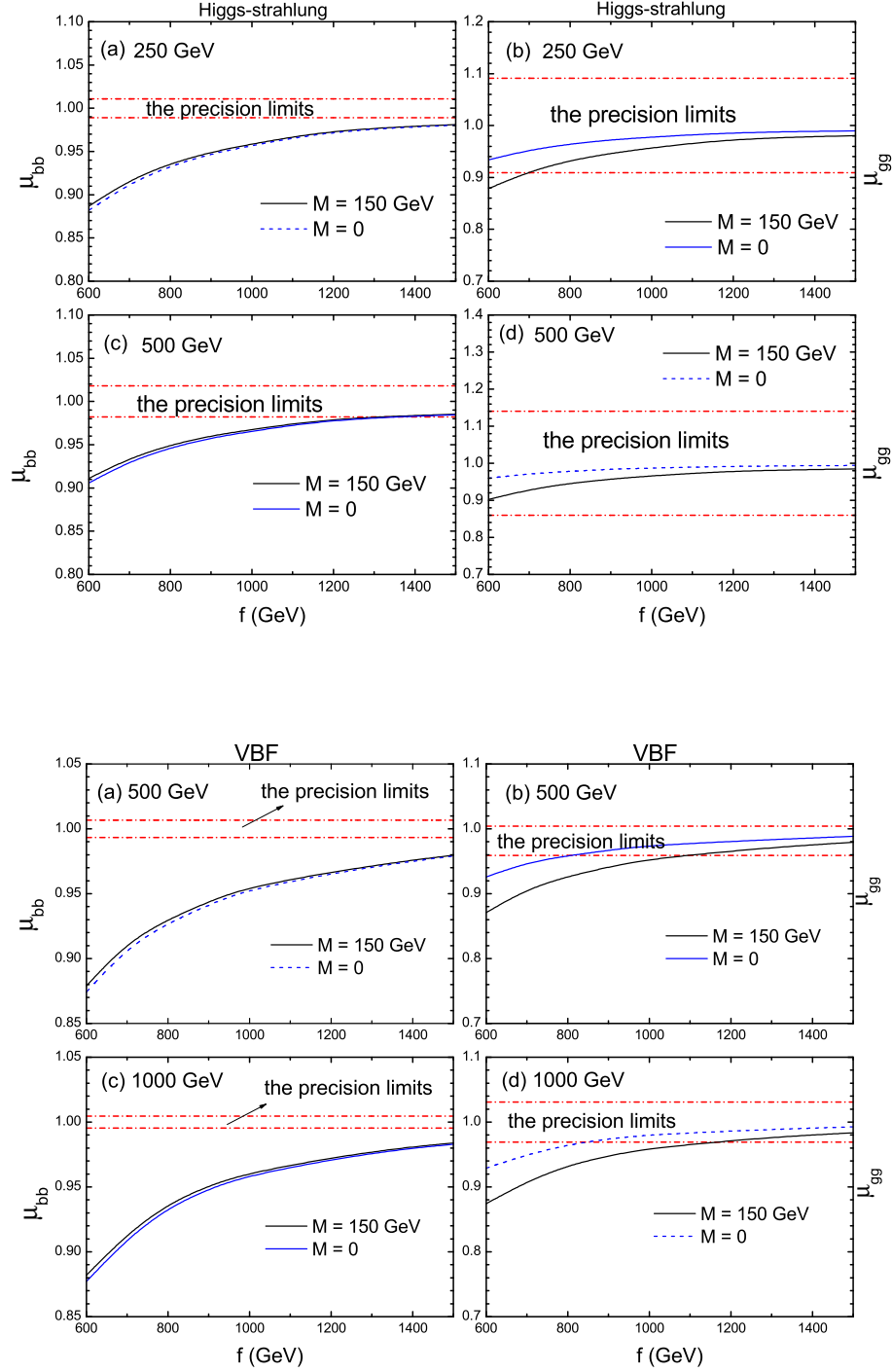


FIG. 6. Higgs signal strengths μ_i ($i = b\bar{b}, gg$) for the processes $e^+e^- \rightarrow Zh$ (upper sub-figures) and $e^+e^- \rightarrow \nu\bar{\nu}h$ (lower sub-figures) as a function of the model scale f at the ILC with polarized beams. The dot-dashed red lines represent the experimental precision limits around the SM expectation according to Table I.

where σ_i denotes the 1σ uncertainty for the signal i in Table 1. In our evaluations, we take $\chi^2 - \chi_{min}^2 \leq 6.18$, where χ_{min} denotes the minimum of χ which happens for the largest values of the parameters f and M , i.e. for $M = 150$ GeV and $f = 1500$ GeV, $\chi_{min}^2 = 3.33$ with the numbers in Table I for the case of ILC-250 GeV, and $\chi_{min}^2 = 14.98$ with the numbers in Table I for the case of ILC-500 GeV, respectively. These samples correspond to the 95% confidence level regions in any

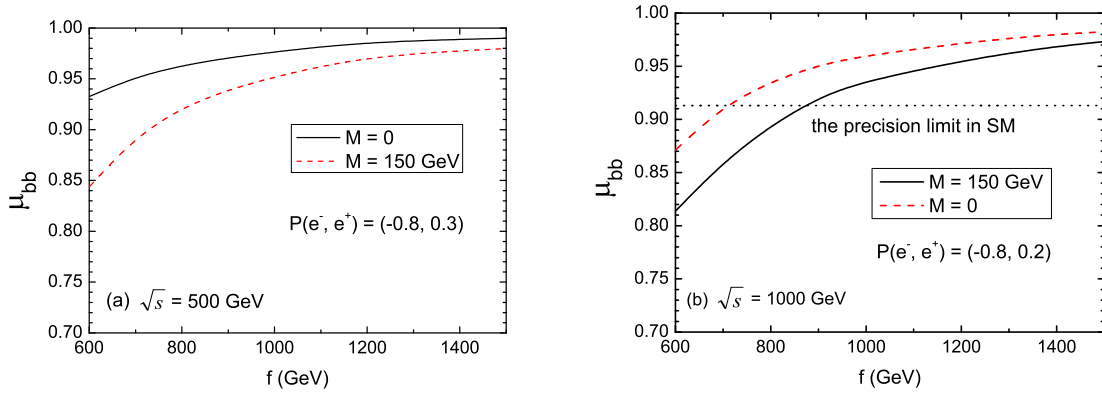


FIG. 7. Higgs signal strengths $\mu_{b\bar{b}}$ for the process $e^+e^- \rightarrow t\bar{t}h$ as a function of the parameter f and M at the ILC with polarized beams for $\sqrt{s} = 500$ and 1000 GeV.

two dimensional plane of the model parameters when explaining the Higgs data.

In Fig. 8 we show the allowed region for parameters M and f at the 2σ level for the cases of ILC-250 GeV, ILC-500 GeV and ILC-1000 GeV, respectively. One can see that (i) the constraint has a rather weak dependence on the variation of the parameter M ; and (ii) the allowed region of the scale parameter f for the case of the ILC-1000 GeV become much narrow than that for ILC-250 GeV. At the 2σ level, for example, the value of f must be larger than 1400 GeV for ILC-1000 GeV, while the lower limit is 1150 GeV for the cas of ILC-250 GeV. The above bounds from the proposed ILC measurements may be much stronger than that for the LHC Higgs data [24].

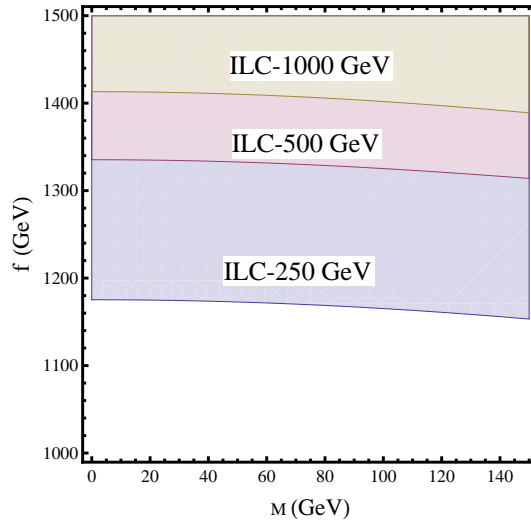


FIG. 8. The allowed region for parameters f and M are shown at the 2σ level for the cases of ILC-250 GeV, ILC-500 GeV and ILC-1000 GeV, respectively.

IV. CONCLUSIONS

The LRTHM is a concrete realization of the twin Higgs mechanism, which provides an alternative solution to the little hierarchy problem. In this work, we studied three Higgs boson production processes $e^+e^- \rightarrow Zh$, $e^+e^- \rightarrow \nu\bar{\nu}h$ and $e^+e^- \rightarrow t\bar{t}h$ in the framework of the LRTHM. We calculated the production cross sections for three processes with and without the polarized beams, the relative corrections with the polarized beams for three energy stages. We also studied the signal rates with the SM-like Higgs boson decaying to $b\bar{b}$ and gg , and performed a simulation by using the projected 1σ sensitivities as listed in Table I. Our numerical results show that:

1. For the considered three processes, the production cross sections with polarized beams are larger than those with unpolarized beams, which are more sensitive to the LRTHM;
2. In a large part of the allowed parameter space, the LRTHM can generate moderate contributions to the HS and VBF processes. For the process $e^+e^- \rightarrow t\bar{t}h$, we found that in certain regions of parameter space (for larger M and lower values of the scale f), the absolute value of the Higgs signal strength $\mu_{b\bar{b}}$ can deviate from the SM prediction by over 8.7%, and thus may be detectable at the future ILC for $\sqrt{s} = 1$ TeV with polarized beams $P(e^-, e^+) = (-0.8, 0.2)$.
3. The future ILC experiments can give strong limit on the scale parameter f . For the case of ILC-250 (1000) GeV, the value of f must be larger than 1150 (1400) GeV at the 2σ level.

ACKNOWLEDGMENTS

We would like thank Shufang Su for providing the CalcHep Model Code. This work is supported by the National Natural Science Foundation of China under the Grant No. 11235005, the Joint Funds of the National Natural Science Foundation of China (U1304112), and by the Project on Graduate Students Education and Innovation of Jiangsu Province under Grant No. KYZZ-0210.

-
- [1] G. Aad et al. (ATLAS Collaboration), **Phys.Lett. B** **716** (2012) 1; **Phys.Lett. B** **726**, 120 (2013).
 - [2] S. Chatrchyan et al. (CMS Collaboration), **Phys.Lett. B** **716** (2012) 30; S. Chatrchyan et al. (CMS Collaboration), **JHEP** **1306** (2013) 081.
 - [3] Plenary talk by M. Kado, "Phyiscis of the Brout-Englert-Higgs boson in ATLAS", ICHEP 2014, Spain.
 - [4] Plenary talk by A. David, "Phyiscis of the Brout-Englert-Higgs boson in CMS", ICHEP 2014, Spain.
 - [5] R. Barbieri and A. Strumia, **Phys.Lett. B** **462** (1999) 144.
 - [6] Z. Chacko, H. S. Goh and R. Harnik, **JHEP** **0601** (2006) 108.
 - [7] Z. Chacko, H. S. Goh and R. Harnik, **Phys.Rev.Lett.** **96** (2006) 231802; Z. Chacko, Y. Nomura, M. Papucci and G. Perez, **JHEP** **0601** (2006) 126;
 - [8] S. Dawson, A. Gritsan, H. Logan, et al., arXiv:1310.8361 [hep-ex]; T. Han, Z. Liu and J. Sayre, **Phys.Rev. D** **89**, (2014) 113006; M. E. Peskin, arXiv:1312.4974 [hep-ph]; P. Bechtle, S. Heinemeyer, O. Stal, T. Stefaniak, G. Weiglein, **JHEP** **1411**, (2014) 039; C. Englert, A. Freitas, M. Muhlleitner, T. Plehn, M. Rauch, M. Spira and K. Walz, **J.Phys. G** **41**, (2014) 113001.

- [9] G. Aarons et al., [ILC Collaboration], arXiv:0709.1893 [hep-ph]; J. Brau et al., [ILC Collaboration], arXiv: 0712.1950 [physics.acc-ph]; T. Behnke, J. E. Brau, B. Foster et al., arXiv:1306.6327 [physics.acc-ph].
- [10] D. M. Asner, T. Barklow, C. Calancha et al., arXiv:1310.0763 [hep-ph].
- [11] H. Ono, A. Miyamoto, **Eur.Phys.J. C** **73** (2013) 2343; E. Boos, V. Bunichev, M. Dubinin, Y. Kurihara, arXiv:1402.4143 [hep-ph]; F. Borzumati, E. Kato, arXiv:1407.2133 [hep-ph].
- [12] J. Fleischer and F. Jegerlehner, **Nucl.Phys. B** **216** (1983) 469; A. Denner, J. Kublbeck, R. Mertig and M. Bohm, **Z. Phys. C** **56** (1992) 261; C. Englert and M. McCullough, **JHEP** **1307** (2013) 168.
- [13] J. R. Ellis, M. K. Gaillard, D. V. Nanopoulos, **Nucl.Phys. B** **106** (1976) 292; B. W. Lee, C. Quigg and H. B. Thacker, **Phys.Rev. D** **16** (1977) 1519; W. Kilian, M. Kramer, P. M. Zerwas, **Phys.Lett. B** **373** (1996) 135; M. Beneke et al., hep-ph/0003033; M. McCullough, **Phys.Rev. D** **90** (2014) 015001; N. Liu, J. Ren, L. Wu, P. Wu, J.M. Yang, **JHEP** **1404** (2014) 189.
- [14] H. Eberl, W. Majerotto, V. C. Spanos, **Phys.Lett. B** **538** (2002) 353; T. Hahn, S. Heinemeyer and G. Weiglein, **Nucl.Phys. B** **652** (2003) 229; G. J. Gounaris and F. M. Renard, **Phys.Rev. D** **90** (2014) 073007; S. L. Hu, N. Liu, J. Ren, L. Wu, **J.Phys. G** **41** (2014) 125004; J. Cao, C. Han, J. Ren, L. Wu, J. M. Yang, Y. Zhang, arXiv:1410.1018 [hep-ph]; N. Craig, M. Farina, M. McCullough, M. Perelstein, **JHEP** **1503** (2015) 146; M. McGarrie, G. Moortgat-Pick, S. Porto, **Eur.Phys.J. C** **75** (2015) 150.
- [15] C.-X. Yue, S.-Z. Wang, D.-Q. Yu, **Phys.Rev. D** **68** (2003) 115004; C.-X. Yue and N. Zhang, **EPL** **77** (2007) 51003; B. Yang, J. Han, S. Zhou and N. Liu, **J.Phys. G** **41** (2014) 075009.
- [16] D. Lopez-Val, J. Sola, N. Bernal, **Phys.Rev. D** **81** (2010) 113005; Y.-B. Liu, J.-F. Shen, H.-M. Han, **EPL** **81** (2008) 31001; J.-F. Shen, J. Cao, L.-B. Yan, **EPL** **91** (2010) 51001; J. Cao, Z. Heng, D. Li, L. Shang, P. Wu, **JHEP** **1408** (2014) 138; D. Barducci, S. de Curtis, S. Moretti, and G. M. Pruna, **JHEP** **1402** (2014) 005; S. Kumar, P. Poullose, arXiv:1408.3563 [hep-ph];
- [17] H.-S. Goh and S. Su, **Phys.Rev. D** **75** (2007) 075010.
- [18] J.-Y. Lee, D.-W Jung, hep-ph/0701071.
- [19] H.-S. Goh and C. A. Krenke, **Phys.Rev. D** **76** (2007) 115018; A. Abada and I. Hidalgo, **Phys.Rev. D** **77** (2008) 113013; P. Batra, Z. Chacko, **Phys.Rev. D** **79** (2009) 095012.
- [20] J. Han, B. Yang, X. Zhang, **EPL** **105** (2014) 31001; Y.-B. Liu, **Phys.Lett. B** **698** (2011) 157; Y.-B. Liu and X.-L. Wang, **Nucl.Phys. B** **839** (2010) 294; L. Wang, L. Wu, J. M. Yang, **Phys.Rev. D** **85** (2012) 075017.
- [21] W. Ma, C.-X. Yue and Y.-Z. Wang, **Phys.Rev. D** **79** (2009) 095010; Y.-B. Liu and X.-L. Wang, **EPL** **86** (2009) 61002; W. Ma, C.-X. Yue and T.-T. Zhang, **Chin. Phys. C** **35** (2011) 333.
- [22] Y.-B. Liu and Z.-J. Xiao, **JHEP** **1402** (2014) 128; Y.-B. Liu and Z.-J. Xiao, **Nucl.Phys. B** **892** (2015) 63.
- [23] L. Wang, X.-F. Han, **Phys.Lett. B** **696** (2011) 79; L. Wang, X.-F. Han, **Nucl.Phys. B** **850** (2011) 233.
- [24] Y.-B. Liu, S. Cheng and Z.-J. Xiao, **Phys.Rev. D** **89** (2014) 015013.
- [25] E. M. Dolle and S. Su, **Phys.Rev. D** **77** (2008) 075013; L. Wang, J. M. Yang, **JHEP** **1005** (2010) 024; Y.-B. Liu and Z.-J. Xiao, **J.Phys. G** **42** (2015) 055004.
- [26] K. A. Olive et al., [Particle Data Group collaboration], **Chin. Phys. C** **38** (2014) 090001.
- [27] G. Aad et al. (ATLAS Collaboration), **JHEP** **1211** (2012) 094; **Phys.Lett. B** **712**, 22 (2012); **Phys.Rev. D** **86**, 012007 (2012); S. Chatrchyan et al. (CMS Collaboration), **JHEP** **1301** (2013) 154. **Phys.Lett. B** **718**, 307 (2012).
- [28] T. Aaltonen et al., (CDF Collaboration), **Phys.Rev.Lett.** **102** (2009) 031801; V.M. Abazov et al., (D0 Collaboration), **Phys.Lett. B** **695** (2011) 88; J. Beringer et al., (Particle Data Group collaboration), **Phys.Rev. D** **86** (2012) 010001; S. Chatrchyan et al., (CMS Collaboration), **Phys.Lett. B** **720** (2013) 63.

- [29] G. Aad et al. (ATLAS Collaboration), **Phys.Lett. B** 718 (2013) 1284.
- [30] G. Aad et al., (ATLAS Collaboration), **JHEP** **1301** (2013) 116.
- [31] S. Chatrchyan et al., (CMS Collaboration), **Phys.Rev. D** **87** (2013) 072002.
- [32] J. Erler, P. Langacker, S. Munir and E. Rojas, **JHEP** **0908** (2009) 017.
- [33] G. Aad et al. (ATLAS Collaboration), **Phys.Rev. D** **90** (2014) 052005.
- [34] Y.-B. Liu, W.-Q. Zhang, L.-B. Yan, **Sci China Phys Mech & Astron** **55** (2012) 757.
- [35] A. Pukhov et al., hep-ph/0412191; A. Belyaev, N. D. Christensen and A. Pukhov, **Comput. Phys. Commun.** **184** (2013) 1729.
- [36] T. Abe et al. [American Linear Collider Working Group Collaboration], hep-ex/0106058.
- [37] G. Moortgat-Pick, T. Abe, G. Alexander et al., **Phys. Rept.** **460** (2008) 131 [hep-ph/0507011].
- [38] N. Arkani-Hamed, A. G. Cohen and H. Georgi, **Phys.Lett. B** **513** (2001) 232; N. Arkani-Hamed, A. G. Cohen, T. Gregoire and J. G. Wacker, **JHEP** **0208** (2002) 020; N. Arkani-Hamed, A. G. Cohen, E. Katz and A. E. Nelson, **JHEP** **0207** (2002) 034; T. Han, H. E. Logan, B. McElrath and L. T. Wang, **Phys.Rev. D** **67** (2003) 095004.
- [39] H. C. Cheng and I. Low, **JHEP** **0309** (2003) 051; H. C. Cheng and I. Low, **JHEP** **0408** (2004) 061; I. Low, **JHEP** **0410** (2004) 067.
- [40] I. Anderson, S. Bolognesi, F. Caola et al., **Phys.Rev. D** **89** (2014) 035007.
- [41] M. E. Peskin, arXiv:1207.2516 [hep-ph]; H. Baer, T. Barklow, K. Fujii et al., arXiv:1306.6352 [hep-ph].